Valence fluctuations and quasiparticle multiplets in plutonium chalcogenides and pnictides

Chuck-Hou Yee,* Gabriel Kotliar, and Kristjan Haule
Department of Physics & Astronomy, Rutgers University, Piscataway, New Jersey 08854-8019, USA
(Received 2 December 2009; published 11 January 2010)

The spectra of Pu chalcogenides and pnictides are computed with dynamical mean field theory within the local density approximation (LDA+DMFT) and interpreted with the aid of valence histograms and slave-boson calculations. We find the chalcogenides are mixed-valent (n_f=5.2) materials with a strongly T-dependent low-energy density of states and a triplet of quasiparticle peaks below the Fermi level. Furthermore, we predict a doublet of reflected peaks above the Fermi level. In the pnictides, the raising of f^6 states relative to f^5 suppresses valence fluctuations, resulting in integral-valent (n_f=5.0) local-moment metals.

DOI: 10.1103/PhysRevB.81.035105 PACS number(s): 71.27.+a, 75.30.Mb

I. INTRODUCTION

The stark contrast in behavior between the plutonium monochalcogenides and monopnictides is a longstanding issue in strongly correlated physics. The pnictides (PuSb, PuAs, and PuP) are comparatively simple metals[1] with embedded f moments arising from trivalent Pu ions which order in the range T_c=85 to 126 K.[2] In contrast, the chalcogenides (PuTe, PuSe, and PuS) exhibit seemingly contradictory behavior: they have a large room-temperature specific heat,[3] yet the resistivity indicates a small gap.[4–6] Also, their lattice constant rules out the full-shell divalent Pu state, yet the susceptibility shows no evidence of Curie-Weiss behavior.[2] Furthermore, photoemission observes a triplet of peaks (the "photoemission triplet") near the Fermi level[7–10] whose origin is still hotly debated.[7,8]

The contrast between the Pu chalcogenides and pnictides exemplifies the view that the Pu 5f electrons sit at the edge of a localization-delocalization transition, where small changes in their electronic environment can drive a transition to itinerancy or localization, thus posing a major challenge to electronic-structure methods. Theoretical studies of the chalcogenides within local-density approximation (LDA) (Refs. 11 and 12) predict a metal and do not account for the photoemission triplet. Methods treating correlations beyond LDA have improved the situation but cannot fully integrate the available experimental data within a single theory. Non-charge self-consistent LDA plus DMFT with FLEX (Ref. 13) predicts metallic behavior and misses the photoemission triplet. Adding charge self-consistency[14] opens a gap but still misses the photoemission triplet. LDA+DMFT with either exact diagonalization in a small Hilbert space[15] or Hubbard-I[16] as the impurity solver describes the photoemission triplet but fails to explain the resistivity.

In this paper, we elucidate the mechanism driving the electronic trends between the pnictides and chalcogenides within a single framework. We find that the chalcogenides are mixed-valent compounds where valence fluctuations combine with the underlying Pu atomic multiplet structure to drive the formation of a multiplet of many-body quasiparticle peaks (quasiparticle multiplets) which correspond to the observed photoemission triplet. These heavy quasiparticles strongly affect the density of states at the Fermi level as a function of temperature, corroborating the gaplike resistivity and large specific heat at room temperature. Using analytic methods, we provide a description of the quasiparticle multiplet formation and their coexistence with the development of a gap. In contrast, the chemistry of the pnictides shifts the atomic multiplet energies, rendering valence fluctuations too costly, thereby localizing the f electrons.

II. NUMERICAL METHOD AND RESULTS

We use LDA+DMFT (Refs. 17 and 18) with OCA (Ref. 19) as the impurity solver to model the chalcogenides and pnictides, taking PuTe and PuSb as representatives of the two groups due to the special attention[1,4,6,7,10] accorded to them in the available experimental data. In our calculations, we use the projective orthogonalized linear muffin-tin orbital basis set.[20] We use F^0=4.5 eV for the Hartree component of the Coulomb interaction, consistent with previous work.[21–23] The remaining Slater integrals F^2=6.1 eV, F^4=4.1 eV, and F^6=3.0 eV are calculated using Cowan's atomic structure code[24] and reduced by 30% to account for screening. The double-counting energy is taken to be $E_{DC}=U(n_f^0-1/2)-J(n_f^0-1)/2$, where n_f^0=5 is the central f valence. We want to emphasize that identical correlations are applied to PuTe and PuSb, which translates to using a single set of atomic parameters F^n and E_{DC} for all computations. The differences in physics originate entirely from changing the alloying element from Te to Sb in the chemical structure.

In Fig. 1, we show the computed spectral functions for PuTe and PuSb, resolution broadened by 40 meV and overlaid with experimental photoemission data.[10] The calculations clearly corroborate the presence of the photoemission triplet in PuTe at the correct energies, and their absence in PuSb. Furthermore, we predict the existence of a doublet of peaks (arrows) in PuTe at reflected energies about the Fermi level. The strong temperature dependence of all five peaks indicates they are quasiparticle resonances. Examining the main quasiparticle peak at the Fermi level (Fig. 2), we find it is composed of heavily renormalized quasiparticles with $Z\approx 0.1$, giving a greatly enhanced specific heat. Additionally, the peak sharpens with decreasing temperature, considerably reducing the density of states at the Fermi level, leading to the formation of a gap and the observed temperature dependence in the specific heat.[3] Together, the reduction in Fermi-level density and heavy renormalization explain how a gap-

 ©2010 The American Physical Society

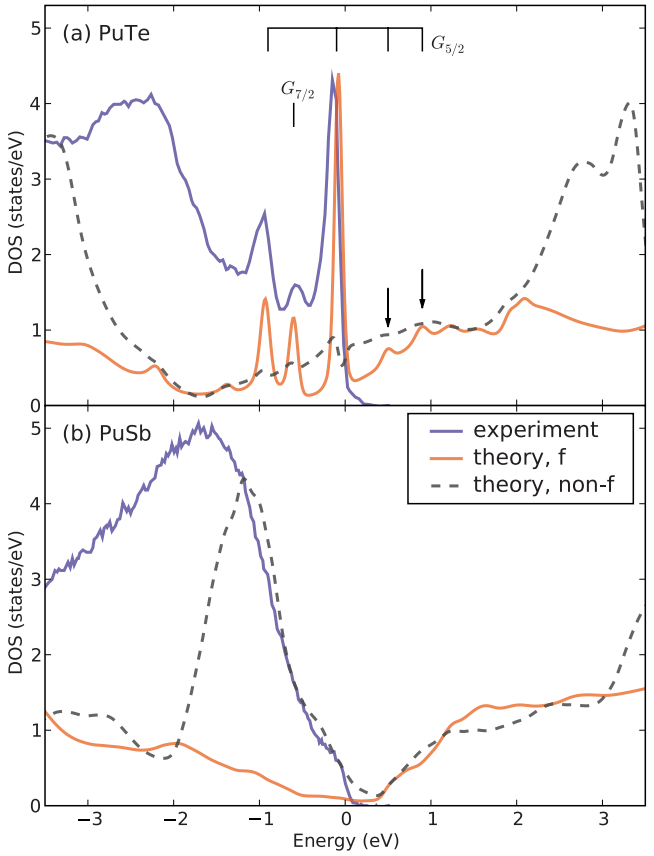

FIG. 1. (Color online) Computed spectra for (a) PuTe and (b) PuSb, separated into f and non-f (uncorrelated spd) partial densities, compared with photoemission (Ref. 10). A triplet of peaks are present in PuTe, as well as a predicted reflected doublet of peaks (arrows), while neither appear in PuSb. Application of broadening (40 meV) has blurred the gap in PuTe (see Fig. 2).

like resistivity can coexist with a large specific-heat coefficient at room temperatures.

A useful way to analyze the Pu atomic environment is to quantify the amount of time the f electrons spend in each

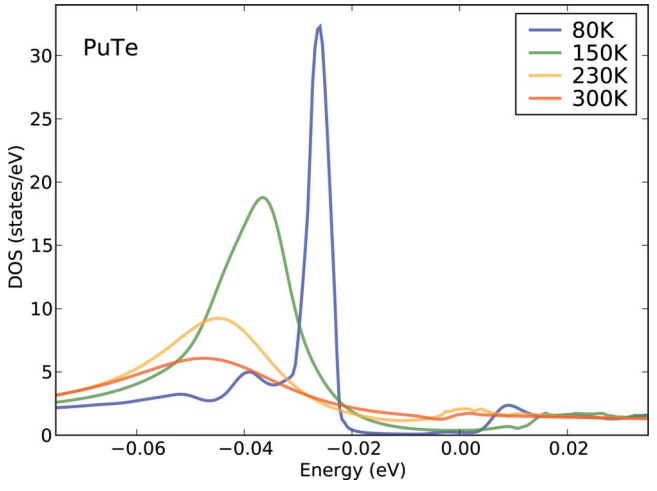

FIG. 2. (Color online) Detail of PuTe spectrum near Fermi level, showing development of gap and formation of main quasiparticle peak with decreasing temperature.

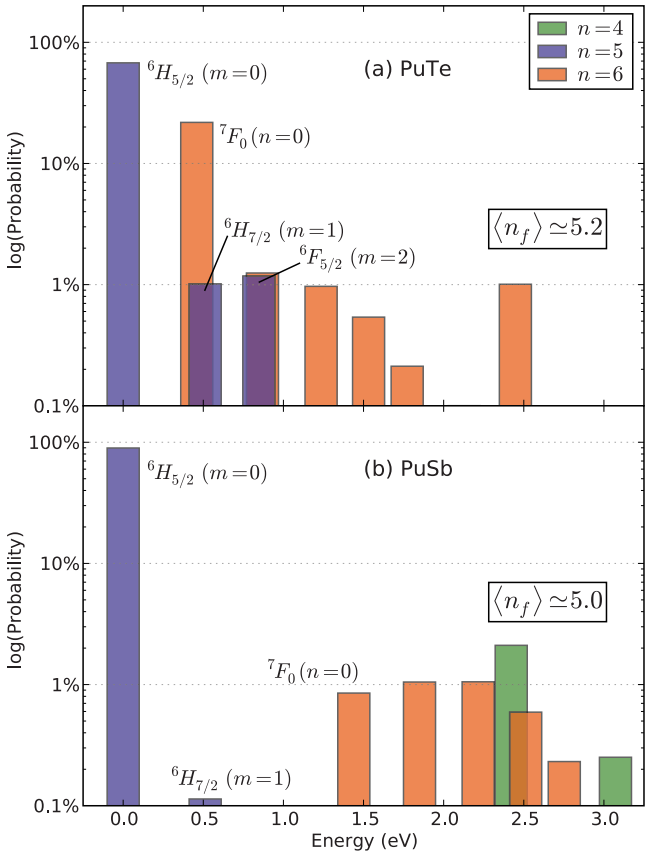

FIG. 3. (Color online) Valence histograms obtained by projection of DMFT solution (T=60 K) onto Pu atomic eigenstates plotted with energies relative to lowest-energy atomic state. The height of each bar represents the percentage of time the atom spends in each configuration. PuTe is strongly mixed valent due to the small energy cost (≈0.5 eV) of valence fluctuations from f^5 to f^6 while PuSb is integral valent due to the large cost of fluctuations to both f^4 and f^6. In PuTe, additional fluctuations to atomic multiplets $^6H_{7/2}$ and $^6F_{5/2}$ are crucial to the creation of the photoemission triplet. All quantum numbers are gathered into a single index m or n used in the slave-boson calculation. Approximate term symbols are given although L and S strictly are not good quantum numbers.

atomic configuration as they fluctuate between the atom and conduction band. To this end, we project the DMFT ground state $|\Omega\rangle$ onto the Pu f-electron atomic eigenstates, resulting in the probabilities $P_m = Z^{-1}\langle\Omega|X_{mm}|\Omega\rangle$, where $Z = \Sigma_m \langle\Omega|X_{mm}|\Omega\rangle$ is the normalization and X_{mm} is the Hubbard operator which projects onto the mth atomic eigenstate.[23] Plotting P_m against the atomic energies gives a valence histogram (Fig. 3) which graphically represent the relative weights of the atomic configurations comprising $|\Omega\rangle$. The f valence can then be defined by $\langle n_f \rangle = \Sigma_m P_m n_m$, where n_m is the number of electrons in the mth state.

The histograms show that the Pu atom is restricted to just one or two valences in both compounds. In fact, the atom mostly exists in a single f^5 configuration ($^6H_{5/2}$, tall blue bar), which we loosely call the "ground state." However, PuTe differs from PuSb in that its electrons have an over 20% probability to fluctuate to the lowest f^6 state ($^7F_0$, leftmost red bar) due to this state's small 0.5 eV separation from

the ground state. The resulting mixed-valent ($\langle n_f \rangle = 5.2$) Pu atom strongly suggests a Kondo-type, and thus nonmagnetic, ground state in PuTe. Additionally, the proximity in energy of the next two higher f^5 states ($^6H_{7/2}$ at 0.5 eV and $^6F_{5/2}$ at 0.9 eV) renders these multiplets accessible to valence fluctuations, which will play a role in generating the photoemission triplet. In contrast, the Pu atom is integral-valent ($\langle n_f \rangle = 5.0$) in PuSb. Within LDA, the $j=5/2$ f bands are higher in energy in PuSb, raising the energy of the f^6 states relative to the f^5. The resulting 1.5 eV gap locks Pu into the lowest f^5 state and PuSb remains a local-moment metal.

III. SLAVE-BOSON ANALYSIS

To gain additional insight into the LDA+DMFT solution, we construct a Hamiltonian for the DMFT quantum impurity. The histograms indicate we only need to keep two valences in the atomic Hilbert space for a low-energy model,

$$H_{\text{atom}} = \sum_m E_m^f f_m^\dagger f_m + \sum_n E_n^b b_n^\dagger b_n, \tag{1}$$

where the auxiliary fermions $f_m^\dagger|0\rangle = |m;f^5\rangle$ and bosons $b_n^\dagger|0\rangle = |n;f^6\rangle$ create the atomic eigenstates, and E_m^f and E_n^b are the corresponding atomic eigenenergies. The Hamiltonian is supplemented by the constraint $Q = \Sigma_m f_m^\dagger f_m + \Sigma_n b_n^\dagger b_n = 1$ in the same spirit as the slave-boson construction.[25,26] The atom hybridizes with an auxiliary conduction bath,

$$H_{\text{c,mix}} = \sum_{k\alpha} \epsilon_{k\alpha} n_{k\alpha} + \sum_{k\alpha} (V_{k\alpha} d_\alpha^\dagger c_{k\alpha} + \text{H.c.}), \tag{2}$$

where $d_\alpha^\dagger$ creates an electron in the αth atomic crystal-field basis and k is the dispersion of the conduction bath. Since we work in the atomic eigenbasis, we eliminate $d^\dagger$ in favor of the auxiliary particles by expanding $d_\alpha^\dagger = b_n^\dagger (F^{\alpha\dagger})_{nm} f_m$, where $(F^{\alpha\dagger})_{nm} = \langle n|d_\alpha^\dagger|m\rangle$ are the matrix elements of the physical electron creation operator.

This model is equivalent to the slave-boson treatment of the multiorbital Anderson impurity model,[27,28] so we can compute the mean-field solution and fluctuations. At the mean-field level, we replace the bosonic operators by their averages, $\langle b_n^\dagger \rangle^2 = \langle b_n \rangle^2 \equiv z_n$ which are the probabilities of the f^6 atomic states (red bars in Fig. 3). Then, the physical Green's function is

$$G_{\alpha'\alpha}(i\omega) = \sum_{m'n'nm} F_{m'n'}^{\alpha'} (F^{\alpha\dagger})_{nm} \sqrt{z_{n'} z_n} G_{m'm}^f(-i\omega), \tag{3}$$

where the auxiliary f propagator and hybridization are

$$G^f(i\omega)_{m'm}^{-1} = (i\omega - E_m^f - \lambda)\delta_{m'm} + i\Delta_{m'm}\ \text{sgn}\ \omega, \tag{4}$$

$$\Delta_{m'm} = \sum_{n'n\alpha} F_{m'n'}^{\alpha} (F^{\alpha\dagger})_{nm} \sqrt{z_{n'} z_n} \Delta_{\alpha\alpha}, \tag{5}$$

and the hybridization $\Delta_{\alpha\alpha'}$ is approximated as an energy-independent constant. Here, λ is the Lagrange multiplier used to maintain $\langle Q \rangle = 1$. The crucial minus sign $G_{m'm}^f(-i\omega)$ arises because the propagation of a physical electron $\sim\langle d(\tau) d^\dagger \rangle$ corresponds to an f hole.

In the Kondo regime, the mean-field equations give

$$T_K \simeq D e^{-\pi(\langle E^b \rangle - E_0^f)/\Delta_{00}/z} \prod_{m\neq 0} \left(\frac{D}{E_m^f - E_0^f} \right)^{\Delta_{mm}/\Delta_{00}}, \tag{6}$$

where $z = \Sigma_n z_n$ is the total f^6 probability and $\langle E^b \rangle = z^{-1} \Sigma_n E_n^b z_n$ is the weighted average of the f^6 energy levels. We ignored the off-diagonal components of $G_{m'm}^f$, which are negligible compared to the diagonal components when $|E_{m'}^f - E_m^f| \gg \Delta_{m'm}$. In the Kondo regime, $\lambda \approx -E_0^f$, pinning the lowest f propagator near the Fermi level.

For PuTe, we explicitly evaluate the sum in Eq. (3) to determine the origin of the photoemission triplet. Keeping just $z_0 \approx 0.20$ since the remaining z_n are negligible (see Fig. 3), we find that only three matrix elements have significant weight: $F_{00}^{5/2}$, $F_{02}^{5/2}$, and $F_{01}^{7/2}$. Again ignoring off-diagonal terms, we find for the physical Green's function

$$G_{5/2}(\omega) = z_0 |F_{00}^{5/2}|^2 G_{00}^f(-\omega) + z_0 |F_{02}^{5/2}|^2 G_{22}^f(-\omega), \tag{7}$$

$$G_{7/2}(\omega) = z_0 |F_{01}^{7/2}|^2 G_{11}^f(-\omega). \tag{8}$$

The selection rules contained in the matrix elements determine the spin-orbit structure of the spectrum: $G_{5/2}$ contains the main peak at the Fermi level and the weaker peak at -0.9 eV (labeled by brackets in Fig. 1) while $G_{7/2}$ contributes the third peak at -0.5 eV. Plugging in $D=1.0$ eV and $\Delta_{5/2} = \Delta_{7/2} = 0.04$ eV into Eq. (6) gives $T_K \approx 500$ K in PuTe, so the peaks have sufficient width to be seen in photoemission. Numerical solution of the mean-field equations with a small hybridization gap, $\Delta_{\alpha\alpha}(\omega) = \Delta_{\alpha\alpha}[\theta(\omega - E_g) + \theta(-\omega - E_g)]$, confirms that for $2E_g \lesssim T_K$, the resonances are not destroyed. Thus, in PuTe, valence fluctuations create three Kondo peaks in the DMFT quantum impurity with spacings determined by the underlying atomic multiplets, corresponding to the quasiparticle triplet in the lattice.

Proceeding to PuSb, the decrement in valence allows Pu to fully transfer three electrons to the pnictogen and exist purely in a trivalent state. Energetically, this is accomplished by raising the f^6 multiplets with respect to the f^5 states, inducing a fourfold increase in $\langle E^b \rangle - E_0^f$ from 0.5 to 2.0 eV. This exponentially suppresses the Kondo temperature of PuSb to under 1 K, eliminating the Kondo peaks, localizing the f electrons and allowing magnetically ordered states at low temperature.

To explain the Hubbard bands and reflected doublet of peaks above the Fermi level, we compute corrections to the mean-field solution. These corrections show that the bare atomic multiplets generate Hubbard bands, which are too broad to be seen in Fig. 1. We emphasize that the photoemission triplet is not directly attributed to atomic multiplets but rather to quasiparticles. Additionally, the corrections to mean field show that the reflected doublet of peaks arises from overlap of the ground-state Kondo singlet with two excited Kondo singlets (Fig. 4). While the ground state is primarily a singlet formed between f_0 and a conduction electron, the two excited states are singlets formed with f_1 and f_2 in place of f_0. Since the atomic multiplets f_1 and f_2 lie at energies 0.5 and 0.9 eV above f_0, the two excited Kondo singlets lie at these energies as well. To generate the spectrum, an electron

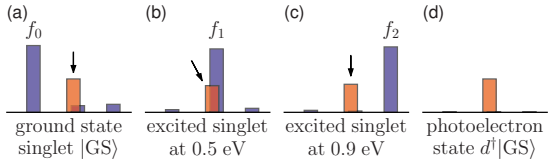

FIG. 4. (Color online) Valence histograms of states responsible for the predicted doublet of peaks above the Fermi level in PuTe. Histograms (a)–(c) depict the ground state and two excited Kondo singlets, respectively. All three state have significant f^6 weight (arrows) due to strong valence fluctuations. Histogram (d) is the photoelectron state $d^\dagger|\mathrm{GS}\rangle$ generated by the addition of an electron to the ground state. Since $d^\dagger$ destroys f_m and creates $b^\dagger$, the result is a state which is entirely f^6 in character. The large f^6 admixture in the excited singlets means they will overlap strongly with the photoelectron state, giving rise to the doublet of peaks at 0.5 and 0.9 eV.

is first added to the ground-state singlet to create a photoelectron state [Fig. 4(d)], which is overlapped with the excited singlets. The overlap is nonzero since all states have an f^6 component due to valence fluctuations, resulting in a doublet of reflected peaks.

IV. SUMMARY

Our LDA+DMFT calculations account for the complex trends observed in experiment across the Pu chalcogenides and pnictides. These include the formation of a low-temperature gap at the Fermi level accompanied by quasiparticle multiplets in the photoemission spectrum. Our theory elucidates the mechanism for the emergence of the quasiparticle multiplet excitations. These excitations represent the remnants of the atomic structure in the low-energy spectra, which is entirely described in terms of quasiparticles. The spectra and f occupancy confirm that the chalcogenides are correlated low-carrier materials in the mixed-valent regime. The chemistry of the pnictides increases the cost of fluctuations and renders the pnictides divalent, thereby eliminating the quasiparticle multiplets.

Our theory has several experimental consequences for the chalcogenides: there should be a quasiparticle doublet at positive energies 0.5 and 0.9 eV which can be probed by inverse photoemission techniques. Furthermore, the quasiparticle multiplets can be detected as side peaks in the optical conductivity, again at 0.5 and 0.9 eV. It would be interesting to study the temperature dependence of both the photoemission and optics near the coherence temperature (500 K) as we expect strong temperature dependence due to the many-body nature of the quasiparticle multiplets. Finally, the mechanism we outline is fairly general and applies to other correlated materials, provided the coherence temperature is large enough to be observed and less than the atomic multiplet splitting.

ACKNOWLEDGMENTS

C.Y. acknowledges useful discussions with P. Coleman. This work was supported by NSF under Grant No. DMR-0806937 and BES-DOE under Grant No. DE-FG02-99ER45761.

*chuckyee@physics.rutgers.edu

[1] A. Blaise, J. M. Collard, J. M. Fournier, J. Rebizant, J. C. Spirlet, and O. Vogt, Physica B & C **130**, 99 (1985).
[2] G. H. Lander, J. Rebizant, J. C. Spirlet, A. Delapalme, P. J. Brown, O. Vogt, and K. Mattenberger, Physica B & C **146**, 341 (1987).
[3] G. Stewart, R. Haire, J. Spirlet, and J. Rebizant, J. Alloys Compd. **177**, 167 (1991).
[4] P. G. Therond, A. Blaise, J. M. Fournier, J. Rossat-Mignod, J. C. Spirlet, J. Rebizant, and O. Vogt, J. Magn. Magn. Mater. **63-64**, 142 (1987).
[5] J. Fournier, E. Pleska, J. Chiapusio, J. Rossat-Mignod, J. Rebizant, J. Spirlet, and O. Vogt, Physica B **163**, 493 (1990).
[6] V. Ichas, J. C. Griveau, J. Rebizant, and J. C. Spirlet, Phys. Rev. B **63**, 045109 (2001).
[7] T. Gouder, F. Wastin, J. Rebizant, and L. Havela, Phys. Rev. Lett. **84**, 3378 (2000).
[8] L. Havela, T. Gouder, F. Wastin, and J. Rebizant, Phys. Rev. B **65**, 235118 (2002).
[9] P. Wachter, Solid State Commun. **127**, 599 (2003).
[10] T. Durakiewicz, J. J. Joyce, G. H. Lander, C. G. Olson, M. T. Butterfield, E. Guziewicz, A. J. Arko, L. Morales, J. Rebizant, K. Mattenberger, and O. Vogt, Phys. Rev. B **70**, 205103 (2004).
[11] P. M. Oppeneer, T. Kraft, and M. S. S. Brooks, Phys. Rev. B **61**, 12825 (2000).
[12] A. O. Shorikov, A. V. Lukoyanov, M. A. Korotin, and V. I. Anisimov, Phys. Rev. B **72**, 024458 (2005).
[13] L. V. Pourovskii, M. I. Katsnelson, and A. I. Lichtenstein, Phys. Rev. B **72**, 115106 (2005).
[14] M.-T. Suzuki and P. M. Oppeneer, Phys. Rev. B **80**, 161103(R) (2009).
[15] A. Svane, Solid State Commun. **140**, 364 (2006).
[16] A. Shick, J. Koloren, L. Havela, V. Drchal, and T. Gouder, EPL **77**, 17003 (2007).
[17] G. Kotliar, S. Y. Savrasov, K. Haule, V. S. Oudovenko, O. Parcollet, and C. A. Marianetti, Rev. Mod. Phys. **78**, 865 (2006).
[18] K. Held, Adv. Phys. **56**, 829 (2007).
[19] K. Haule, S. Kirchner, J. Kroha, and P. Wölfle, Phys. Rev. B **64**, 155111 (2001).
[20] A. Toropova, C. A. Marianetti, K. Haule, and G. Kotliar, Phys. Rev. B **76**, 155126 (2007).
[21] S. Y. Savrasov, G. Kotliar, and E. Abrahams, Nature (London) **410**, 793 (2001).
[22] J.-X. Zhu, A. K. McMahan, M. D. Jones, T. Durakiewicz, J. J. Joyce, J. M. Wills, and R. C. Albers, Phys. Rev. B **76**, 245118 (2007).
[23] J. H. Shim, K. Haule, and G. Kotliar, Nature (London) **446**, 513 (2007).
[24] R. D. Cowan, *The Theory of Atomic Structure and Spectra* (University of California Press, Berkeley, 1981).

[25] P. Coleman, Phys. Rev. B **29**, 3035 (1984).
[26] G. Kotliar and A. E. Ruckenstein, Phys. Rev. Lett. **57**, 1362 (1986).
[27] N. E. Bickers, D. L. Cox, and J. W. Wilkins, Phys. Rev. B **36**, 2036 (1987).
[28] J. Kroha, S. Kirchner, G. Sellier, P. Wölfle, D. Ehm, F. Reinert, S. Hüfner, and C. Geibel, in 23rd International Conference on Low Temperature Physics (LT23) [Physica E (Amsterdam) **18**, 69 (2003)].